

Performance of Prototype of Optically Readout TPC with a ^{55}Fe source

I. Abritta Costa^a, E. Baracchini^b, F. Bellini^{a,c}, L. Benussi^d,
S. Bianco^d, G. Cavoto^{a,c}, E. Di Marco^a, G. Maccarrone^d,
M. Marafini^e, G. Mazzitelli^d, A. Messina^{a,c}, D. Piccolo^d, D. Pinci^a,
F. Renga^a, F. Rosatelli^d and S. Tomassini^d

^a Istituto Nazionale di Fisica Nucleare, Sezione di Roma, I-00185, Italy

^b Gran Sasso Science Institute L'Aquila, I-67100, Italy

^c Dipartimento di Fisica, Sapienza Università di Roma, I-00185, Italy

^d Istituto Nazionale di Fisica Nucleare, Laboratori Nazionali di Frascati, I-00040, Italy

^e Museo Storico della Fisica e Centro Studi e Ricerche "Enrico Fermi", Piazza del Viminale 1, Roma, I-00184, Italy

E-mail: emanuele.dimarco@roma1.infn.it

Abstract. The performances of an optical readout of Time Projection Chambers (TPCs) with multiple Gas Electron Multipliers (GEMs) amplification stages are presented. The detector is characterized by using a ^{55}Fe source within a 7 litre sensitive volume detector in different electric field configurations. This prototype is developed as a part of the R&D for the CYGNO project for an application to direct Dark Matter search through the detection of tracks of nuclear recoils in the gas within the keV energy range.

1. Experimental setup and data analysis

All measurements described in this work were carried out on a prototype for the future CYGNO experiment, called Large Elliptical MOdule (LEMON, Fig. 1) which is described in details in refs. [1, 2, 3].

The main elements of LEMON are:

- A sensitive volume (A) filled with 7 litre of He/CF₄ 60/40 gas mixture at atmospheric pressure, surrounded by a field cage (FC) composed of 20 elliptic silver plated wire rings with axes of 24 cm (along x) and 20 cm (along y) and a depth of 20 cm (along z);
- The sensitive volume is closed on one side by a semi-transparent cathode made of a thin wire mesh and on the other side by a structure of three 20×24 cm², 50 μm thick GEMs;
- The whole structure is contained in a gas-tight box with two transparent windows on the cathode and the GEM sides;
- On the cathode side, beyond the window, a fast photo-sensor PMT (B) is placed to readout all the light produced by the GEMs;
- On the other side, downstream to an adjustable bellow (C), an ORCA Flash 4.0 camera, 1.33 × 1.33 cm² scientific CMOS sensor (subdivided in 2048 × 2048 pixels with an active

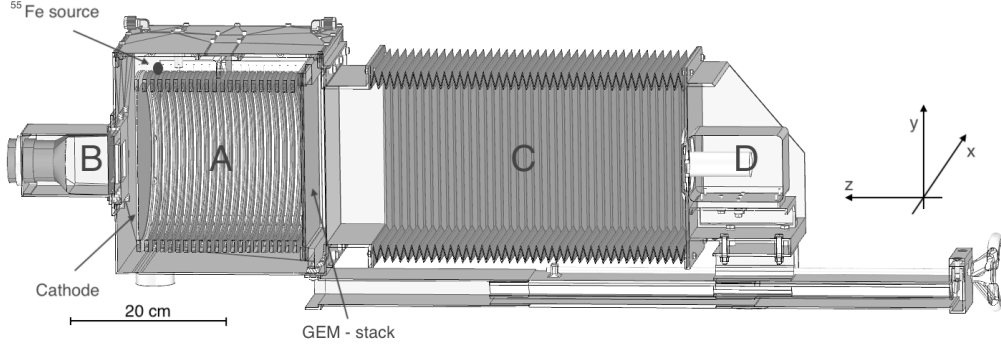


Figure 1. Drawing of the experimental setup. In particular, the elliptical field cage close on one side by the triple-GEM structure and on the other side by the semitransparent cathode (A), the PMT (B), the adaptable bellow (C) and the CMOS camera with its lens (D) are visible.

area of $6.5 \times 6.5 \mu\text{m}^2$ each) and equipped with a Schneider lens distance of 52.5 cm (i.e. 21 Focal Length, FL) for the acquisition of the light produced in the GEM holes. In this configuration, the sensor faces a surface of $26 \times 26 \text{ cm}^2$ and therefore each pixel at an area of $130 \times 130 \mu\text{m}^2$. The geometrical acceptance Ω therefore results to be 1.6×10^{-4} [4].

A ^{55}Fe source, with an activity of about 100 Bq, was placed between two FC rings, 18 cm far from the GEM as shown in Fig. 1. Because of the short distance between the plastic rings supporting the FC wires and their width along the x and y directions, these acted as a collimator for the photons emitted by the source, so that the effective distance from the GEMs of their interactions with the gas molecules was estimated to be 18 ± 2 cm. Electrons produced within the sensitive volume are drifted by the electric field (E_d) present within the FC, toward the GEMs where the multiplication process takes place. Typical operating conditions of the detector are: $E_d = 600 \text{ V/cm}$, an electric field in the GEM produced by $V_{\text{GEM}} = 460 \text{ V}$ for each GEM plane and a transfer field $E_t = 2 \text{ kV/cm}$. The maximum value of (E_d) is limited by the maximum voltage provided by the HV generator (15 kV) used for the measurements reported in this paper.

The results presented in this poster are based on data acquired by the ORCA sensor in free running mode, without any trigger. The light produced during the multiplication processes in the GEM were recorded with an exposure of 100 ms. The analysis algorithm is based on two steps:

- (i) *Pedestal subtraction.* A *blind run* of 100 images was acquired with the sensor in total dark. For each pixel, the pedestal is evaluated as the average number of counts recorded in this run and is subtracted to the counts collected in all recorded images. A sensor noise of 1.9 photons per pixel was measured as rms of the pedestal distribution.
- (ii) *Clustering:* a very simple nearest neighbor-cluster (NNC) clustering algorithm was developed. A lower resolution version of each image was created with *macro-pixels* made by matrices of 4×4 pixels. The average count over the 16 pixels, after subtracting their pedestal values, is assigned to each macro-pixel. A cluster is reconstructed by at least two neighbouring macro-pixels having more than 2 counts (i.e. 2 photons [5]) each.

Figure 2 shows an example of an image of two light spots due the interaction of the ^{55}Fe photons in the gas.

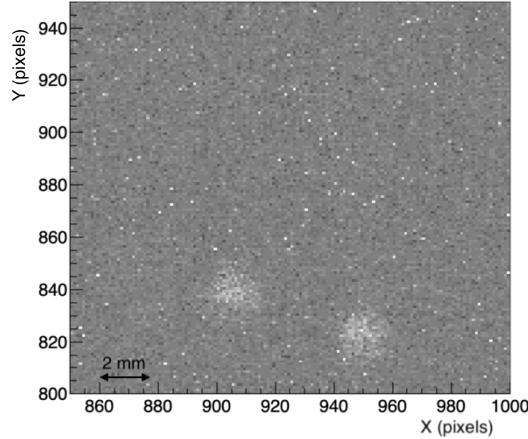


Figure 2. Example of two clusters due to X-ray interaction in gas.

2. Backgrounds

The CMOS sensor used for the measurements has two main sources of noise:

- a dark current of about 0.06 electrons per second per pixel;
- a readout noise of about 1.4 electrons rms (in our set-up it was found to be slightly larger probably due to an effect of *ageing* of the sensor built more than 5 years ago);

The sensor electronic noise represents a possible unavoidable instrumental background and it can generate *ghost-clusters*. The distribution of the light in each *ghost-cluster* found in the *blind run* is shown in Fig. 3 (left).

The shape of the distribution is determined by the positively-definite counts of photons in the cluster. Its shape is used to estimate an operative threshold that allows to suppress fake signals due to sensor noise. The distribution is fitted with an exponential function and the tail extrapolated with this function. From the fitted parameters, and by taking into account that a run lasts 10 s, it is possible to extrapolate the probability of having a *ghost-clusters* with an amount of light larger than a given threshold. As an example, a threshold of 300 photon counts corresponds to 1×10^{-4} *ghost-clusters/second*.

The GEM structure can, in principle, create a diffused light background because of possible micro-discharges. To evaluate it, the distribution of the light in the clusters reconstructed outside the sensitive area was studied. As it is shown in Fig. 3 (right), the obtained distribution is similar to the one due to the sensor electronic noise and has a tail that can be described with an exponential with a slope which is very similar to the one obtained for the sensor noise. The few events found outside the bulk of the distribution are short tracks very likely due to events occurred close to the GEM, where the residual electric field of the GEM is able to capture electrons and drive them toward the multiplication channels.

As already described in Sec. 1, within the FC area an evident diffused and flat background is visible. To study it, a run without the radioactive source was acquired. Superimposing the images of all the reconstructed clusters in the whole run, results into an observed spatial distribution of clusters similar to the one found in presence of the source.

Figure 4 shows 10 overlapped events randomly chosen within the run. They appear as to be mostly tracks due to cosmic rays or low energy electrons from natural radioactivity. In a radio-pure apparatus operating underground such a background is expected to be strongly suppressed. Moreover, pattern recognition should be able to identify and reject residual events. For this reason, the effect of this background is not taken into account in this paper for the evaluation of the possible operative threshold.

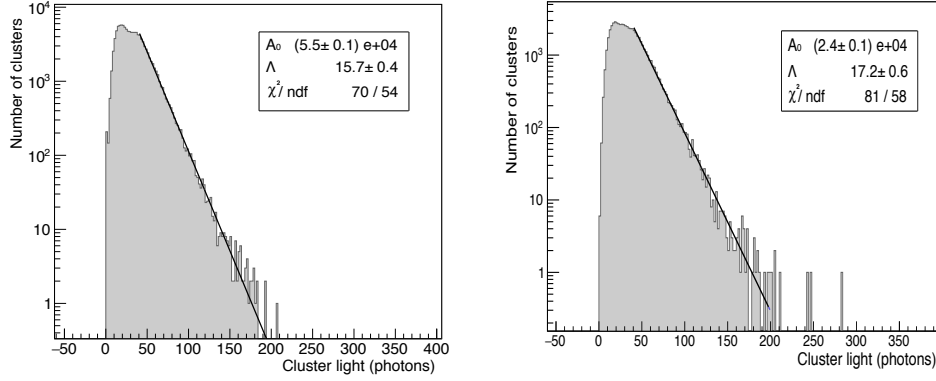


Figure 3. Left: Distribution of the light in clusters reconstructed in a run with blind sensor. Right: distribution of the light recorded clusters reconstructed outside from the sensitive area in a run with ^{55}Fe source with superimposed exponential fit.

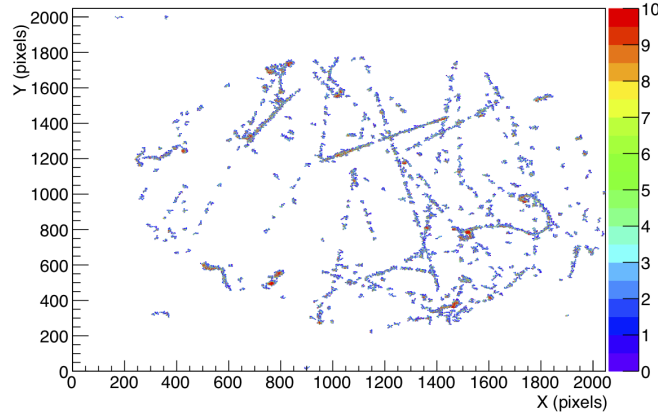


Figure 4. Example of 10 events acquired in a run without the ^{55}Fe source within the detectors. Color scale indicates the number of photons collected per pixel.

3. Cluster size and light spectrum

For each run, the spectrum of the total light in clusters reconstructed within the sensitive area and the distribution of their size (i.e. the number of over-threshold pixels) are studied. Figure 5 shows an example of these distributions for a run taken with $V_{\text{GEM}} = 450$ V, $E_d = 600$ V/cm and $E_t = 2$ kV/cm.

Only clusters with at least 30 pixels over-threshold were considered. The distribution is fitted with the sum of an exponential function to model the background due to natural radioactivity (Sec. 2), and a Polya function, expressed by Eq. 1, often used to describe the response spectrum of MPGD [6]:

$$P(n) = \frac{1}{b\bar{n}} \frac{1}{k!} \left(\frac{n}{b\bar{n}} \right)^k \cdot e^{-n/b\bar{n}} \quad (1)$$

where b is a free parameter and $k = 1/b - 1$. The distribution has \bar{n} as expected value, while the variance is governed by its mean and the parameter b : $\sigma^2 = \bar{n}(1 + b\bar{n})$. From the result of the fits it is possible to evaluate:

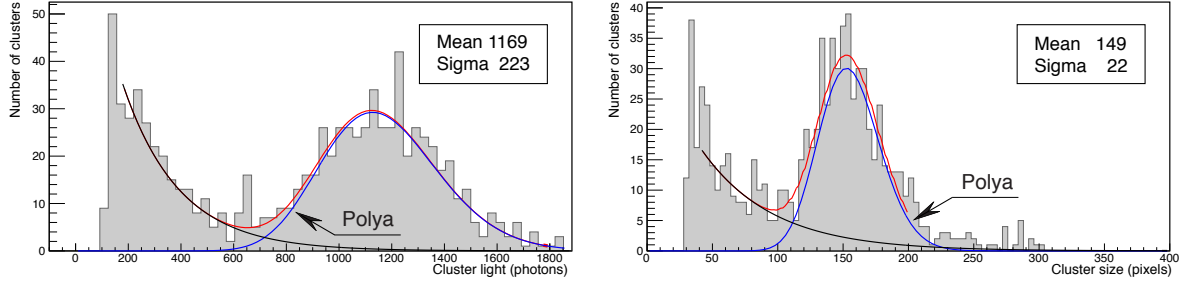


Figure 5. Distribution of total light (left) and number of illuminated pixels (right) for a run taken with $V_{\text{GEM}} = 450$ V, $E_d = 600$ V/cm and $E_t = 2$ kV/cm.

- the expected value of the distribution \bar{n} and its variance σ^2 . These parameters, when fitted on the light distributions, give the detector response in term of number of photons and the energy resolution. The latter will thus indicate the variance (σ) of the Polya fit in the whole paper. When fitting the number of illuminated pixels distribution, the average size of the clusters can be evaluated by taking into account the effective area of $130 \times 130 \mu\text{m}^2$ (see Sect. 1) acquired by each single pixel.
- the integral of the Polya component, that is proportional to the total number of reconstructed clusters and that can be used to evaluate the detection efficiency;

Since, as it is shown on the left of Fig. 5, in this configuration 1169 ± 223 photons are collected per cluster (i.e. each 5.9 keV released), a threshold of 400 photons corresponds to about 2 keV released in the sensitive volume. The average cluster size was found to be 149 pixels (Fig. 5, right).

4. Results

The response of the detector to the ^{55}Fe source has been studied as a function of three different operative parameters: V_{GEM} , E_d and E_t . The results are reported in the following.

(i) Dependence on the voltage applied to the GEM (V_{GEM})

The voltage applied to the GEM (V_{GEM}) determines the gain and therefore the light yield of the structure. Then, the average number of collected photons per cluster and its fluctuations as a function of V_{GEM} is expected to raise increasing V_{GEM} . Figure 6 (left) shows that the detector light yield increases exponentially and doubles every $V_{\text{GEM}} = 30$ V step. The energy resolution is also found not to be significantly dependent on the voltage applied to the GEM with a value around 20%. Both results are found in good agreement with results obtained with similar experimental setup [7].

The cluster size is also found to increase with the GEM photon yield. On the right of Fig. 6, the total amount of the cluster detected normalised to its maximum value is shown. The lower edge of the plateau, at around $V_{\text{GEM}} = 440$ V, is estimated as the minimal voltage to get the detector maximally efficient, with a global efficiency close to unity.

(ii) Dependence on the Drift Field (E_d):

All measurements were taken with the ^{55}Fe source 18 cm away from the readout plane and therefore, the response of the detector as a function of the electric field within the FC (E_d) provides information on the effect of electron attachment and diffusion in our configuration. Fluctuations of the number of photons per cluster (Fig. 7, left) have a small increase for small values of E_d (from around 20% to almost 30%). The detection efficiency (Fig. 7 right) remains well above 95% for E_d larger than 300 V/cm.

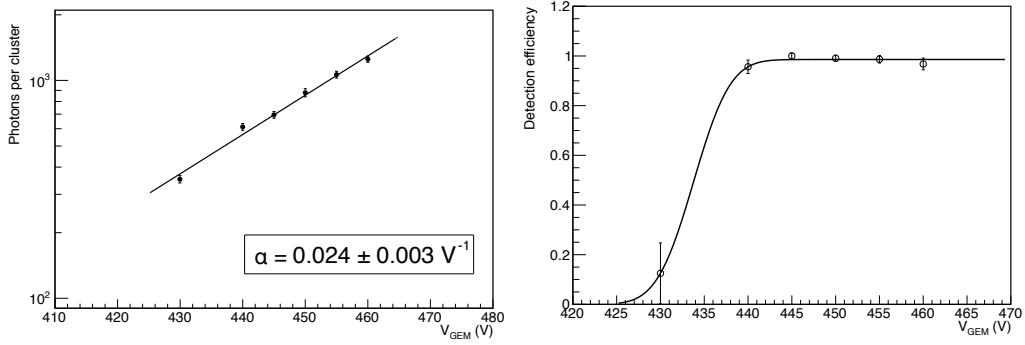


Figure 6. Left: average of the light spectrum with an exponential fit (left) and its relative fluctuations (right) as a function of V_{GEM} for a run taken with $E_d = 600 \text{ V/cm}$ and $E_t = 2 \text{ kV/cm}$. Right: dimension spectra (right) and detection efficiency as a function of V_{GEM} for a run taken with $E_d = 600 \text{ V/cm}$ and $E_t = 2 \text{ kV/cm}$.

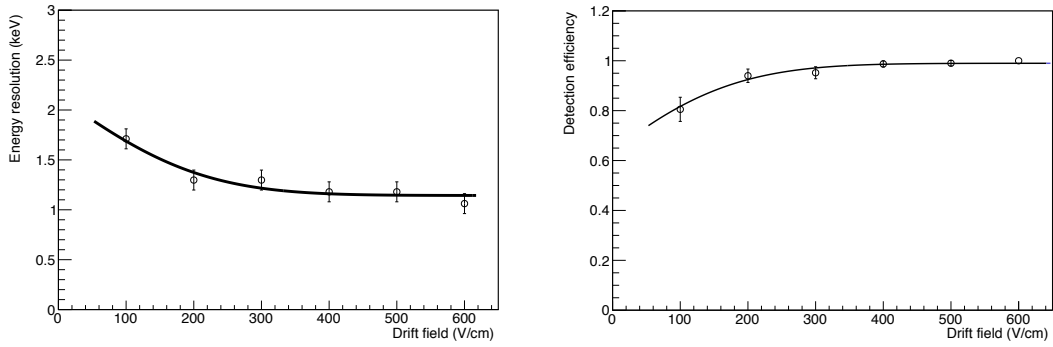


Figure 7. Left: average light spectrum (left) and detection efficiency (right) as a function of E_d for a run taken with $V_{\text{GEM}} = 450 \text{ V}$ and $E_t = 2 \text{ kV/cm}$.

(iii) Dependence on the Transfer Field (E_t)

The electric field in the gap between the GEM, E_t , plays a crucial role in the electron transport and on the effective gain of the detector. Because of a better capability in extracting electrons [8], the number of collected photons increases linearly with the E_t reaching a value of 1200 for $E_t = 2.5 \text{ kV/cm}$ (while their fluctuations are quite stable around 20%). In this configuration, therefore, a sensitivity of 0.2 collected photons per released keV was measured.

5. Conclusion

The analysis of the tests performed on the LEMON detector with the 5.9 keV photons provided an important characterisation of its response. With a suitable field configuration ($V_{\text{GEM}} = 460 \text{ V}$, $E_d = 600 \text{ V/cm}$ and $E_t = 2.5 \text{ kV/cm}$), the response of the detector is measured to be 1200 ph/cluster, i.e 1 photon each 5 released electronvolts. From the studies of the sensor intrinsic noise, it was possible to determine that a threshold of 400 photons ensures a rate of fake events smaller than 10 per year. With a sensitivity of 0.2 ph/eV this would represent a threshold of 2 keV. With an $E_t = 2 \text{ kV/cm}$, the detection efficiency was estimated to be well above 95% down to $V_{\text{GEM}} = 430 \text{ V}$ where 1/3 of light is collected compared to $V_{\text{GEM}} = 460 \text{ V}$ and $E_t = 2.5 \text{ kV/cm}$. Therefore, working with the latter settings would provide 3 more times light and thus,

full detection efficiency seems possible for 2 keV signals.

- [1] Pinci D, Di Marco E, Renga F, Voena C, Baracchini E, Mazzitelli G, Tomassini A, Cavoto G, Antochi V C and Marafini M 2017 *PoS EPS-HEP2017* 077
- [2] Mazzitelli G, Antochi V C, Baracchini E, Cavoto G, De Stena A, Di Marco E, Marafini M, Pinci D, Renga F, Tomassini S and Voena C 2017 *2017 IEEE Nuclear Science Symposium and Medical Imaging Conference (NSS/MIC)* pp 1–4 ISSN 2577-0829
- [3] Mazzitelli G, Antochi V C, Baracchini E, Cavoto G, De Stena A, Di Marco E, Marafini M, Pinci D, Renga F, Tomassini S and Voena C 2018 *2018 IEEE Nuclear Science Symposium and Medical Imaging Conference (NSS/MIC)* vol Under publication in IEEE Nuclear Science Symposium Medical Imaging Conference, 2018
- [4] Marafini M, Patera V, Pinci D, Sarti A, Sciubba A and Torchia N M 2018 *IEEE Transactions on Nuclear Science* **65** 604–608
- [5] Marafini M, Patera V, Pinci D, Sarti A, Sciubba A and Spiriti E 2015 *JINST* **10** P12010 (*Preprint* 1508.07143)
- [6] Blum W, Rolandi L and Riegler W 2008 *Particle detection with drift chambers* Particle Acceleration and Detection, ISBN = 9783540766834 ISBN 9783540766834, 9783540766841 URL <http://www.springer.com/physics/elementary/book/978-3-540-76683-4>
- [7] Phan N S, Lee E R and Loomba D 2017 *arXiv 1703.09883* (*Preprint* 1703.09883)
- [8] Pinci D 2006 *A triple-GEM detector for the muon system of the LHCb experiment* Ph.D. thesis Cagliari University, CERN-THESIS-2006-070 URL <http://weblib.cern.ch/abstract?CERN-THESIS-2006-070>